MRS Advances © 2019 Materials Research Society
DOI: 10.1557/adv.2019.6

Transferring Microelectromechanical Devices to Breathable Fabric Carriers with Strain-Engineered Grippers

Sushmita Challa[1], Canisha Ternival[2], Shafquatul Islam[1], Jasmin Beharic[1], Cindy Harnett[1]

[1]*University of Louisville J.B. Speed School of Engineering, 2210 S Brook St, Louisville, KY 40208, U.S.A.*

[2]*University of Florida*

ABSTRACT
Stretchable electronics fabrication generally relies on fine-tuning adhesion forces, putting some restrictions on what the carrier layer can be. In contrast to adhesion, mechanical tangling makes more kinds of carrier materials available. Antibacterial, conductive, heat-responsive and other functions can be brought in by fiber networks as long as they are compatible with the highly selective silicon etch process. Mechanical grippers can also bring electronic contacts from one side of a mesh to the other, which is difficult to do on continuous thin films of other soft materials like silicone or polyimide. Our solution uses mechanical strain to produce large arrays of redundant grippers from planar thin-film designs.

INTRODUCTION:

The convergence of wearable and stretchable electronic technologies has pushed microfabricated devices toward new carrier materials, device architectures, and mechanics [1]. Stretchable carrier materials such as the elastomer poly(dimethylsiloxane) (PDMS) and other silicones offer low modulus responses to large strain deformations. But there are challenges. Consider that the modulus of silicon is 10^5 times as high as a typical elastomer; and the thermal expansion coefficient is 10^2 times smaller [2]. The elasticity mismatch is solved by making devices from thin, flexible films, and creating meandering paths that bend instead of break when stretched. Could the same structures transfer to porous, fiber-based carrier materials instead of silicone? Fabrics offer lightweight mechanical support and high conduction of air and fluids, an advantage for wearable sensors, but the contact region is non-uniform compared to a cast silicone film. For this reason, adhesion and other printing based methods to transfer thin film devices from wafers to fabrics may be difficult to control. In the present work, we investigate mechanical tangling as a way to adhere MEMS devices onto fabric carriers.

Strain-engineered microfabricated grippers wrap around the mesh during the final step in our microfabrication process. Applications include sensor integration into breathable structures like tissue engineering scaffolds, bandages, and filters.

The proposed fiber based carrier materials could contribute to electronic textiles (E-textiles), a rapidly emerging field. Smart materials are incorporated into E-textiles by embroidering [3], knitting [4], weaving [5], spinning [6], braiding [7], coating/laminating [8], printing [9] and chemical treatments [10]; mechanical tangling at the microlevel adds a new tool to the E-textiles suite. Our approach uses micro-origami which has become widespread due to numerous applications including biomedical devices, [11] energy storage systems, optoelectronics, MEMS, [12] metamaterials, bendable microelectronics, and origami nanorobots [13].

Three-dimensional out of plane structures have previously been assembled from two-dimensional patterns by several different phenomena producing a wide variety of shapes. Surface tension as described by Gagler [14] and Gracias et al. [15-16, 17, 18, 19] can form boxes or pyramids at the microscale [20-, 21, 22, 23]. To produce coiled cantilevers, nano-scrolls and tubes [24- 25, 26, 27, 28] through micro and nano-origami, mismatched tensile and compressive stresses in bilayers is employed. Differential thermal expansion or a lattice size mismatch between layered materials can cause released bimorphs to curl uniformly from the substrate. [29] The magnitude of the force, elastic moduli, and the thickness of the film decide the curvature of the bilayer objects. The direction of rolling or folding of the patterns is controlled by stresses, shape, and direction of etching. [29] Adhesion forces [30] and collision with other objects can change the shape of the structures—an expected outcome when the grippers interact with fabric fibers. In the present work, mechanical tangling between thin-film devices and fiber materials is achieved by strain-mismatched bilayer curling. Grippers were made from thin-film bilayers on a silicon wafer. At the final release step, the grippers curled up and interacted with fabrics. In the following sections, we analyze the gripper design, fabrication, testing, results and future research.

DESIGN:

Transferring our microfabricated structures to fabrics via secure mechanical joints requires fiber wrapping, preferably more than halfway around. By depositing metal at below 200 C on a silicon dioxide (SiO_2) layer grown at 1000 C, strain mismatched bimorphs are created. The upper metal film constrains the expansion of the lower SiO_2 layer thus when released from the substrate, the bilayer curls with a radius of curvature that minimizes its potential energy. Our previous work [29] produced curvature radii in the 60 to 100 micron range. In the present work, we created radial arrays of gripper arms with lengths in the 200 micron range (Figure 1).

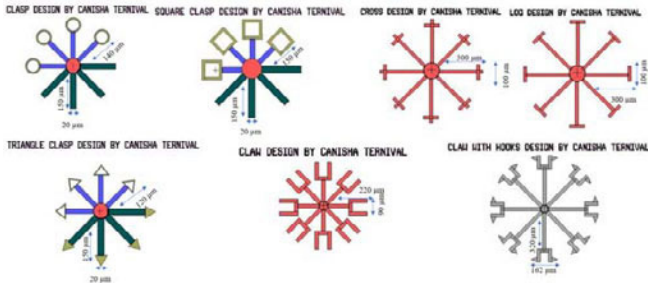

Figure 1: Grippers with arm lengths in the range of 200 microns drawn in L-Edit microelectronic layout software.

The radius of curvature for reliable clasping depends on the fabric being clasped; most of the fabrics we studied had fibers in the 50 to 100 micron diameter range. The reciprocal of radius of curvature for a released gripper arm of uniform width is given by, [29]

$$\frac{\mathbf{1}}{\boldsymbol{\rho}} = \frac{\mathbf{6}\varepsilon\mathbf{(1+m)^2}}{\boldsymbol{d}[\mathbf{3(1+m)^2+(1+mn)\{m^2+(mn)^{-1}\}}]} \ldots (\mathbf{1}) = \frac{\mathbf{6}\varepsilon \boldsymbol{d_1 d_2}}{\boldsymbol{d^3}} \ldots (\mathbf{2})$$

Equation (1) reduces to equation (2), if both layers have same biaxial moduli. [1] In the above equation, $\boldsymbol{\rho}$ is the radius of curvature, $\boldsymbol{d = d_1 + d_2}$, combined thickness of two layers, $\boldsymbol{n}$ is the ratio of the elastic modulus of the two layers $(\boldsymbol{E_1/E_2})$ and m is the ratio of their thicknesses, $(\boldsymbol{d_1/d_2})$, ε is the strain mismatch given as follows,

$$\varepsilon = \frac{\sigma_{Metal}(1-\nu_{Metal})}{E_{Metal}} - \frac{\sigma_{oxide}(1-\nu_{Oxide})}{E_{Oxide}} \quad (3)$$

where σ is the biaxial stress, ν is the Poisson's ratio, E is the elastic modulus. The choice of the thickness of upper metal layer in the bimorph greatly affects the radius of curvature. From equation (1), with a SiO_2 layer thickness of 400nm, and other parameters as listed in Table 1, the following plot showing radius of curvature versus thickness of upper metal layer is obtained (Figure 2).

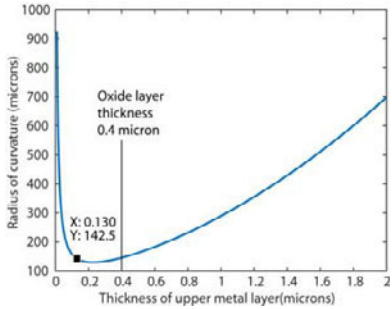

Figure 2: Plot of radius of curvature versus thickness of upper metal layer from Equation (1), using the parameters in Table 1. The minimum radius occurs when the metal layer is approximately half the thickness of the oxide.

Table 1: Properties of the bilayer used in this work

Material	**Elastic Modulus (GPa)**	**Poisson's Ratio**	**Measured Thickness (nm)**	**Measured Residual Stress (MPa)**	**Calculated Radius (microns)**
Cr	$E_{Metal} = 140$	$\nu_{Metal} = 0.21$	130	$\sigma_{Metal} = 160 \pm 5$ (tensile)	142±5
Oxide	$E_{Oxide} = 71$ $E_{Oxide} = 83$	$\nu_{Oxide} = 0.20$	400	$\sigma_{oxide} = -300 \pm 25$ (Compressive)	

METHODS:

Fabrication

Fabrication proceeded as shown in Figure 3. A 400 nm thick thermal oxide was grown on silicon wafers by wet oxidation in a tube furnace at 1000 C. Standard photolithography and etching were used to pattern Cr metal into the designs of Figure 1. To produce the metal thickness and stress values in Table 1, a sputtering machine (Lesker PVD75) was used to sputter coat the wafers from a Cr target using 300 W DC power, 5 mTorr argon pressure and 15–18 minutes of deposition time. The oxide was removed by plasma etching everywhere except where it was protected by the metal pattern. For achieving this, wafer dices were processed in a March plasma etcher for 10 minutes with 240 mTorr pressure of CF4:H2 at a partial pressure ratio of 60:40 and a RF power of 260 W.

Fabrics (Matte Tulle Fuschia 100% nylon, Casa Collection Chiffon Chocolate 100% polyester, Glitterbug Micronet Fabric White 100% nylon, Jo Ann Fabrics) were attached tightly over the surface, then the structures were released using a XeF_2 etch chamber (Xactix, Inc.) to undercut them from the wafer by a 10 micron deep isotropic silicon etch. For grippers with arm widths in the range of 15 microns, the etch process required 30 or more 30 s cycles of exposure to an atmosphere of 3 Torr XeF_2 for complete release.

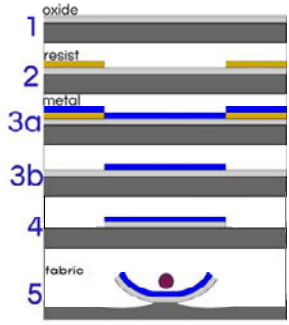

Figure 3: (1) Thermal oxide deposition (2) Pattern with photolithography (3a) Chromium deposition by sputtering (3b) Metal lift-off in NMP solvent (4) Wafer dicing and oxide etching using the metal as a mask. (5) Fabrics are tightly attached over the chips and silicon is etched by xenon difluoride through the fibers, releasing the structures.

Partial release, leaving grippers tethered to the wafer at their centers, could be achieved by reducing the number of etch cycles. Figure 3 showed the fibers in a cross-sectional view, while Figure 4 illustrates an idealized vision of grippers transferring semiconductor payloads to a fabric swatch, creating a porous structure with mechanical strength coming from fibers and functionality from thin-film devices. Note that in the proof-of-concept work presented here, we rely on random alignment of fibers and grippers.

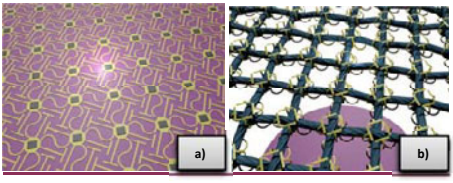

Figure 4: Top view rendering of grippers interacting with fibers a) planar layout b) after release to a grid.

RESULTS:

We used scanning electron microscopy and optical microscopy to evaluate the radius of curvature, as well as whether MEMS devices could realistically be moved from silicon wafers to fabrics using the strain energy based "pop-up" process. Film stress was measured on 4-inch diameter wafers using a Toho film stress monitor. The properties in Table 1 (a 400 nm oxide, and a 130 nm thick Cr layer) produced structures with a radius of curvature ranging from 100 to 193 microns, for an average of 144 ± 41 microns based on measurements from 6 structures. For the fabric transfer process, imperfections included missed connections, too-short grippers, and crushing of grippers by misaligned fabric (Figure 5). Successes showed that the fabric is neither visibly damaged nor does the fabric interfere with MEMS processing (Figure 6). Chemical effects of XeF_2 etching, which can leave a hydrophobic residue on samples in the presence of humidity [31], were not investigated.

Pop-up Errors

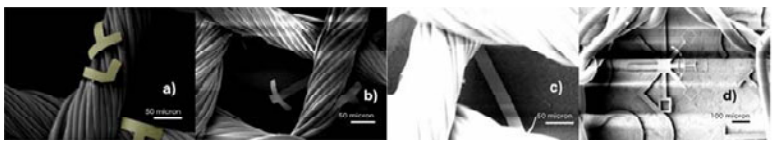

Figure 5: Pop-up Errors: a) broken corners (with yellow highlight to show the MEMS device) b) too-short grippers c) crushing by misaligned fabric; d) missed connections.

Pop-up Success

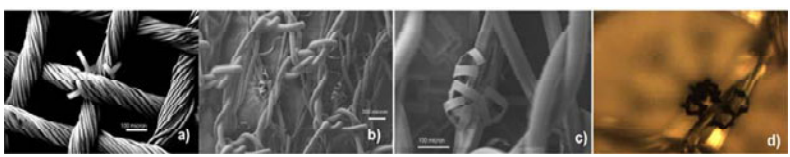

Figure 6: Pop-up Success: Fabric does not interfere with MEMS processing in Figure 3, and fabric is not damaged a) Woven polyester fabric worked b) Knit nylon fabric worked c) Zoom on previous figure showing secure clasping of 50 micron diameter fibers by the "crab claw" design d) Optical micrograph of the knit nylon fabric showing interaction between polymer fibers and bilayer materials.

DISCUSSION

For the materials and thicknesses in Table 1, we have found that structure lengths of 200 microns and greater are sufficient for hooking on polyester and nylon woven and knit

fabrics having fiber diameters in the 50- to 100 micron range, and having mesh openings in the 500 micron to 1 mm diameter range. Features such as crossbars and a "crab claw" (Figure 1, lower center, and Figure 5c) spanned more of the fiber surface; devices that rely on contact area for adhesion should include such features at the ends of the grippers. The three "clasp" designs in Figure 1 were too short (< 200 microns) to surround these fibers at the ~150 micron radius of curvature. Future work includes revisiting the clasp designs with longer arms, doing intentional fiber alignment on linear arrays, and carrying out force measurement during pull testing. The goal is more efficient spatial use of grippers as illustrated in Figure 4. If alignment is not possible, increased gripper density could help achieve a strong bond between a thin film device array and a fabric.

Acknowledgments

We would like to acknowledge financial support from the IMPACT REU program (NSF award 1560235) and Kentucky Science and Engineering Foundation grant KSEF-3503-RDE-019, as well as microfabrication support by Julia W. Aebersold, Curtis P. McKenna, and Evgeniya Moiseeva in the University of Louisville cleanroom.

References:

1. A. Koh, et al., Sci. Transl. Med. **8** (366), 366ra165 (2016)
2. J.A. Rogers, T. Someya, and Y. Huang, Science **327** (5973), 1603 (2010)
3. Popular Embroidery Techniques Used to Decorate Fabrics. Available at: http://nanetteparker.hubpages.com/hub/Popular-Embroidery-Techniques-Used-to-Decorate-Fabrics (accessed 26 September 2018).
4. Creative Sewing. Available at: http://www.creativesewing.co.nz/ (accessed 26 September 2018).
5. Loominous. Available at: http://www.loominous.co.uk/studio.html (accessed 26 September 2018).
6. Cornell University: Fabrics of Our Livelihoods. Available at: http://smallfarms.cornell.edu/2011/07/04/fabrics-of-our-livelihoods/ (accessed 26 September 2018).
7. CMI. Available at: https://www.colonialmills.com/PublicStore/catalog/BraidingProcess,156.aspx (accessed 26 September 2018).
8. Textile Innovation Knowledge Platform. Available at: http://www.tikp.co.uk/knowledge/technology/coating-and-laminating/laminating (accessed 26 September 2018).
9. Custom Fabric Printing. Available at: http://sophiasdecor.blogspot.it/2012/09/insidespoonflower-custom-fabric.html (accessed 26 September 2018).
10. Durable water repellent. Available at: http://en.wikipedia.org/wiki/Durable_water_repellent (accessed 26 September 2018).
11. T. Bozhi, et al., Nat. Mater. **11** (11), 986 (2012)
12. D. Bishop, F. Pardo, C. Bolle, R. Giles and V. Aksyuk, J. Low. Temp. Phys. **169**(5–6), 386 (2012)
13. B.Y. Ahn, E.B. Duoss, M.J. Motala, X. Guo, S.L. Park, Y. Xiong, J. Yoon, R.G. Nazzo, J.A. Rogers and J.A. Lewis, Science **323** (5921), 1590 (2009)
14. R. Gagler, A. Bugacov, B.E. Koel and P.M. Will, J. Micromech. Microeng. **18** (5), 055025 (2008)
15. B. Gimi, T. Leong, Z. Gu, M. Yang, D. Artemov, Z.M. Bhujwalla and D.H. Gracias, Biomed. Microdevices **7** (4), 341 (2005)
16. R. Fernandes and D.H. Gracias, Adv. Drug Deliv. Rev. **64** (14), 1579 (2012)
17. T.G. Leong, P.A. Lester, T.L. Koh, E.K. Call and D.H. Gracias, Langmuir. **23** (17), 8747 (2007)
18. J.H. Cho, A. Azam and D.H. Gracias, Langmuir. **26** (21), 16534 (2010)
19. J.S. Randhawa, S.S. Gurbani, M.D. Keung, D.P. Demers, M.R. Leahy-Hoppa and D.H. Gracias, Appl. Phys. Lett. **96** (19), 191108 (2010)
20. J.H. Cho, M.D. Keung, N. Verellen, L. Lagae, V.V. Moshchalkov, P. Van Dorpe and D.H. Gracias, Small. **7** (14), 1943 (2011)
21. J.C. Breger, C. Yoon, R. Xiao, H.R. Kwag, M.O. Wang, J.P. Fisher, T.D. Nguyen and D.H. Gracias, ACS Appl. Mater. Interfaces. **7** (5), 3398 (2015)
22. V.B. Shenoy and D.H. Gracias, MRS Bulletin. **37** (09), 847 (2012)
23. K. Malachowski, M. Jamal, Q. Jin, B. Polat, C.J. Morris and D.H. Gracias, Nano Lett. **14** (7), 4164 (2014)

24. V. Ya. Prinz, V.A. Seleznev, A.K. Gutakovsky, A.V. Chehovskiy, V.V. Preobrazhenskii, M.A. Putyato and T.A. Gavrilova, Physica E **6** (1), 828 (2000)
25. O.G. Schmidt and K. Eberl, Nature **410** (6825), 168 (2001)
26. M.N. Huang, L. Boone, M. Roberts, D.E. Savage, M.G. Lagally, N. Shaji, H. Qiu, R. Blick, J.A. Nairn and F. Liu, Adv. Mater. **17** (23), 2860 (2005)
27. O.G. Schmidt and N.Y. Jin-Phillipp, Appl. Phys. Lett. **78**, 3310 (2001)
28. P.O Vaccaro, K. Kubota and T. Aida, Appl. Phys. Lett. **78**, 2852 (2001)
29. E. Moiseeva, Y. M. Senousy, S. McNamara, and C. K. Harnett, J. Micromech. Microeng. **17** (9), N63 (2007)
30. L. Malkinski and E. Rahmatollah, Magnetic Materials (InTech, 2016), pp.223-248, Retrieved from intechopen
31. F. I. Chang, R. Yeh, G. Lin, P.B. Chu, E. G. Hoffman, E. J. Kruglick, K. S. J. Pister, and M. H. Hecht, Proc. SPIE **2641**, pp. 117-129 (1995)